

Effect of Graft Chain Length of the Stabilizer on Dispersion Polymerization of Methyl Methacrylate in Petrol

KAJARI KARGUPTA, PURNENDU RAI, and ANIL KUMAR*

Department of Chemical Engineering, Indian Institute of Technology, Kanpur—208 016, India

SYNOPSIS

To carry out dispersion polymerization of methyl methacrylate (MMA) in petrol, we have used a poly(MMA) grafted-poly(12-hydroxystearic acid) copolymer as the stabilizer. This special copolymer was prepared as a solution in a mixture of ethyl acetate and butyl acetate solvents. We investigated the effect of graft chain length of the stabilizer on the dispersion polymerization in petrol. We synthesized the stabilizer copolymer with $n = 1-4$ and determined the rate and the molecular weight of the PMMA formed. There is no dispersion polymerization for $n = 1$. However, for any other n , for a given stabilizer concentration, as the chain length of the graft is increased, the molecular weight as well as the rate of PMMA formation increases. As opposed to this for a given graft length as the concentration of the stabilizer increases, the molecular weight of PMMA first rises, but for a larger concentration, it begins to fall after undergoing a maximum. In this work, we modeled the heterogeneity of the reaction mass and proposed a mathematical model for dispersion polymerization of MMA in petrol. The computer results are found to conform to the experimentally observed molecular weight of the PMMA. © 1993 John Wiley & Sons, Inc.

INTRODUCTION

The nonaqueous dispersions of polymers are found to have higher polymer content compared to those obtained through emulsion polymerization.^{1,2} In addition to this, these dispersions have low viscosity and good shear stability. Since organic solvents have high vapor pressure and low heat of evaporation, they have industrial applications in the coating industry. In addition to this, the other important area of application is the field of electroreprographics as developers and toners. In this, an alkyl acrylate or methacrylate is polymerized in hydrocarbon diluent and the resultant dispersion is compounded with polyethylene wax to produce a wax/acrylic dispersion. The rapid drying characteristics of nonaqueous dispersions is sometimes utilized in printing inks that can be heat-set at considerably lower temperatures. Polymer prepared through nonaqueous polymerization is also utilized for improving the mechanical properties of other polymers, as, for ex-

ample, in the preparation of unscorched polyurethane foams. Dispersions of polymers are frequently mixed into bulk plastics to increase toughness and impact resistance.

In a typical nonaqueous dispersion polymerization, the reactants consist of the reacting monomer (or monomers), a suitable initiator, and stabilizers of the polymer dispersion formed.³⁻¹³ These reactants are dissolved in the reaction medium to form a homogeneous solution. During the course of the reaction, insoluble polymer is formed that precipitates and the nucleation process depends upon the solubility of the polymer in the medium. It also depends upon the concentration of the stabilizer and the effect of monomer upon the solvency of the polymer. During the nucleation of the particle, their numbers increase, but after some time, it has been shown to take an asymptotic value. After the nucleation stage is over, the polymerization enters the second stage in which disappearance of the monomer shows up in the growth of polymer particles. The greatest demand of stabilizer is at the nucleation stage, but only very little is required in the second stage because only very little surface is generated by the growth of the particles.

* To whom correspondence should be addressed.

The most commonly used stabilizers for dispersion polymerization have been block and graft copolymers. The molecular weight of the soluble component of the graft copolymer is usually not critical, but for practical considerations, it must be above 1000–1500. The grafts are chosen such that they form an “anchor” upon the polymer particles. It is observed that in the aqueous phase the hydrophobic end of the emulsifier becomes weakly adsorbed on the surface of the polymer particle. In most organic solvents, this rejection energy is very small, and, as a consequence, the anchor groups are required to be large so as to be sufficiently incompatible as well as insoluble in the medium. However, if this graft chain length is too large, they would tend to form a large cluster of micelles that does not dissociate into single molecules. The latter is needed for them to migrate to the surface of particles so as to provide the necessary stability. A careful balance must therefore be made between the anchor and soluble components of the stabilizer, which is sometimes called the anchor/soluble (or in short, ASB) factor.

The literature is full of studies on aqueous (emulsion or dispersion) polymerization.^{14–27} This is primarily because the emulsifiers used for stabilizing polymer dispersion in the aqueous phase are easily available. The heterogeneous reaction occurring in emulsion polymerization has been modeled rigorously. The oldest mathematical model describing emulsion polymerization is the Smith and Ewart theory. In this, it is assumed that the primary radical could enter into polymer particles. This is a gross simplification because of the thermodynamic limitations of radicals entering into the particles. For several systems, it has been shown that the transfer and termination reactions in the aqueous phase occur significantly and cannot be ignored. Lichti et al. established theories predicting the particle-size distribution (PSD) in emulsion polymerization, which is a matrix partial differential equation and can be solved in the general form numerically only. If we wish to determine the molecular weight distribution (MWD) of the polymer formed, we have to understand the termination processes occurring within the polymer particles.

In this paper, we have systematically studied the dispersion polymerization of methyl methacrylate (MMA) in petrol using poly(MMA)-*g*[poly(12-hydroxyteric acid)] copolymer as the stabilizer. The nature of the stabilizer copolymer was shown to have a considerable effect upon the course of polymerization of MMA in petrol. The stabilizer copolymer was synthesized with varying graft lengths and its effect upon the rate of consumption of MMA and

the molecular weight of the polymer formed was carefully monitored. It was shown that for the graft length of unity there was no dispersion polymerization of MMA; however, as the graft length increased, the rate as well molecular weight of the polymer PMMA increased. For a given graft length of the copolymer stabilizer, an optimal concentration is found showing the ASB effect. Subsequently, a kinetic model has been proposed and the kinetic equations have been derived and solved on a computer. The model equations are found to adequately describe the experimental data.

EXPERIMENTAL

The stabilizer copolymer needed for dispersion polymerization has been prepared using the technique given in Appendix I. The petrol was decolorized using charcoal, and its flash point and boiling characterization were determined as described in Appendix II.

The setup used for dispersion polymerization of MMA in petrol is shown in Figure 1. After the bath temperature is attained, about 9 g of MMA in 300 mL of petrol with about 4 g of benzoyl peroxide were introduced into the reaction vessel. This is done for seeding and the total duration of the seed stage was kept at 30 min for satisfactory dispersion polymerization. After the completion of the seed stage, a monomer feed consisting of 109 g of MMA, 2 g of

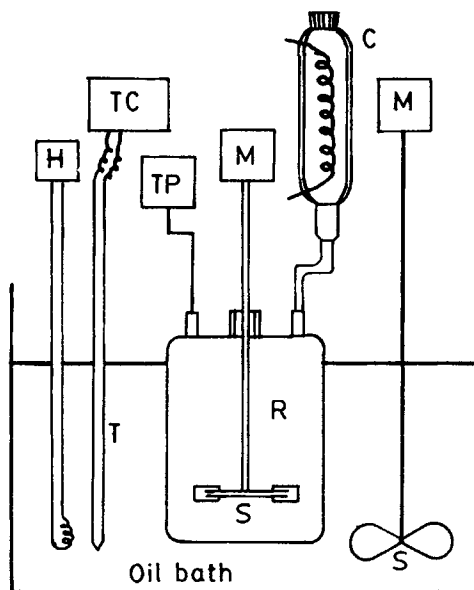


Figure 1 Distribution of phases in the reaction mass.

methacrylic acid, 0.3 g of benzoyl peroxide, and the stabilizer copolymer was prepared. This was fed to the reactor and the dispersion polymerization was carried out for 4 h. Samples of the reaction mass were withdrawn at regular interval of times and were analyzed for the weight of the polymer formed and its viscosity average molecular weight.

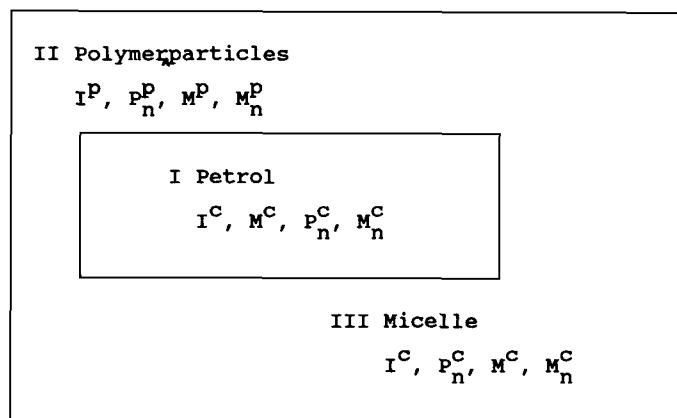
THEORETICAL DEVELOPMENTS

Experimentally, we found that the initiator benzoyl peroxide as well as the monomer MMA mix in all

proportions with petrol. This would mean that in the dispersion polymerization of MMA in petrol the monomer droplets do not exist as a separate phase. It is expected that at the reaction temperature polymer radicals are initiated in the petrol phase and can grow in chain length up to a certain critical value (say n^*). We observe that at any time of polymerization there are the following three phases as given in Figure 2:

1. Continuous petrol phase (denoted by superscript c).
2. Discrete polymer particle phase (denoted by superscript p).

DISTRIBUTION OF PHASES IN THE REACTION MASS



Distribution of Phases	Component Present
I : Continuous phase (Petrol)	Initiator (I^C) Monomer (M^C) Polymer radical (P_n^C) Poly Methyl Methacrylate (M_n^C)
II: Discrete Polymer particle phase ($n < n^*$)	Initiator (I^P) Monomer (M^P) Polymer radical (P_n^P) Poly Methyl Methacrylate (M_n^P)
III: Micelle phases Formed by surfactant molecules	Initiator (I^m) Monomer (M^m) Polymer radical (P_n^m) Poly Methyl Methacrylate (M_n^m)

Figure 2 Experimental setup. H: heater; TP: trap and vacuum pump; M: motor; TC: temperature controller; C: condenser; S: stirrer; T: thermocouple.

Table I Mole Balance Equations of Various Species in the Heterogeneous Polymerization in Organic Medium**For $n < n^*$, $n > 1$:**

$$\frac{1}{V_p} \frac{d}{dt} (V_p [P_n]^p) = 0 = -[P_n]^p \{ K_p^p [M]^p + K_t^p \sum_{j=1}^{\infty} [P_j]^p + K_{trm}^p [M]^p + K_{trp}^p \sum_{j=2}^{\infty} [M_j]^p \} \\ + K_p^p [M]^p [P_{n-1}]^p + K_{trp}^p [M_n]^p \sum_{j=2}^{\infty} [P_i]^p - K_{ma} ([P_n]^p - [P_n]^c) \quad (1)$$

$$\frac{1}{V_0 - V_p} \frac{d}{dt} \{ (V_0 - V_p) [P_n]^c \} = 0 = -[P_n]^c \{ K_p^c [M]^c + K_t^c \sum_{j=1}^{n^*-1} [P_j]^c + K_{trm}^c [M]^c + K_{trp}^c \sum_{j=2}^{n^*-1} [M_j]^c \} \\ + K_p^c [M]^c [P_{n-1}]^c + K_{trp}^c [M_n]^c \sum_{i=1}^{n^*-1} [P_i]^c - K_{ma} ([P_n]^p - [P_n]^c) \quad (2)$$

For $n = 1$:

$$\frac{1}{V_p} \frac{d}{dt} (V_p [P_1]^p) = 0 = K_p^p [I]^p [M]^p + K_{trm}^p M^p \sum_{i=2}^{\infty} [P_i]^p - K_{trp}^p [P_1]^p \sum_{j=2}^{\infty} [M_j]^p - K_p^p [P_1]^p [M]^p \\ - K_t^p [P_1]^p \sum_{i=1}^{\infty} [P_i]^p + K_{ma} [P_1]^c - [P_1]^p \quad (3)$$

$$\frac{1}{(V_0 - V_p)} \frac{d}{dt} \{ (V_0 - V_p) [P_1]^c \} = 0 = K_p^c [I]^c [M]^c + K_{trm}^c [M]^c \sum_{i=2}^{n^*-1} [P_i]^c \\ - K_{trp}^c [P_1]^c \sum_{j=2}^{n^*-1} [M_j]^c - K_p^c [P_1]^c [M]^c - K_t^c [P_1]^c \sum_{i=1}^{n^*-1} [P_i]^c + K_{ma} [P_1]^c - [P_1]^p \quad (4)$$

 $n > n^*$:

$$[P_n]^c = 0 \quad (5)$$

$$-\frac{1}{V_p} \frac{d}{dt} (V [P_n]^p) = 0 = -[P_n]^p \{ K_p^p [M]^p + K_t^p \sum_{j=1}^{\infty} [P_j]^p + K_{trm}^p [M]^p \\ + K_{trp}^p \sum_{j=2}^{\infty} [M_j]^p \} + K_p^p [M]^p [P_{n-1}]^p + K_{trp}^p [M_n]^p \sum_{i=1}^{\infty} [P_i]^p \quad (6)$$

For $n = n^*$:

$$K_p^c [M]^c [P_{n^*-1}]^c + K_{ma} [P_{n^*}]^c = 0 \quad (7)$$

$$-[P_{n^*}]^p \{ K_p^p [M]^p + K_t^p \sum_{j=1}^{\infty} [P_j]^p + K_{trm}^p [M]^p + K_{trp}^p \sum_{j=2}^{\infty} [M_j]^p \} \\ + K_p^p [M]^p [P_{n^*-1}]^p + K_{trp}^p [M_{n^*}]^p \sum_{i=1}^{\infty} [P_i]^p - K_{ma} ([P_{n^*}]^p) = 0 \quad (8)$$

For $n < n^*$:

$$\frac{1}{V_p} \frac{d}{dt} (V_p [M_n]^p) = K_t^p [P_n]^p \sum_{j=1}^{\infty} P_j^p + K_{trm}^p [P_n]^p [M]^p + K_{trp}^p [P_n]^p \sum_{j=2}^{\infty} [M_j]^p \\ + K_{trp}^p M_n^p \sum_{i=1}^{\infty} [P_i]^p - K_{ma} \{ [M_n]^p - [M_n]^c \} \quad (9)$$

$$\frac{1}{V_0 - V_p} \frac{d}{dt} \{ (V_0 - V_p) [M_n]^c \} = K_t^c [P_n]^c \sum_{j=1}^{n^*-1} [P_i]^c + K_{trm}^c [P_n]^c [M]^c \\ + K_{trp}^c [P_n]^c \sum_{j=2}^{n^*-1} [M_j]^c + K_{trp}^c [M_n]^c \sum_{i=1}^{n^*-1} [P_i]^c - K_{ma} \{ [M_n]^c - [M_n]^p \} \quad (10)$$

Table I (Continued)**For $n > n^*$:**

$$[M_n]^c = 0 \quad (11)$$

$$\frac{1}{V_P} \frac{d}{dt} (V_P [M_n]^p) = K_i^p [P_n]^p \sum_{j=1}^{\infty} P_j^p + K_{trm}^p [P_n]^p [M]^p + K_{trp}^p [P_n]^p \sum_{j=2}^{\infty} [M_j]^p - K_{trp}^p M_n^p \sum_{i=1}^{\infty} [P_i]^p \quad (12)$$

For $n = n^*$:

$$\frac{1}{(V_0 - V_P)} \frac{d}{dt} \{ (V_0 - V_P) [M_n^c] = K_{ma} [M_{n^*}]^p \quad (13)$$

$$\begin{aligned} \frac{1}{V_P} \frac{d}{dt} (V_P [M_{n^*}]^p) = & K_i^p [P_{n^*}]^p \sum_{j=1}^{\infty} P_j^p + K_{trm}^p [P_{n^*}]^p [M]^p \\ & + K_{trp}^p [P_{n^*}]^p \sum_{j=2}^{\infty} [M_j]^p - K_{trp}^p M_{n^*}^p \sum_{i=1}^{\infty} [P_i]^p - k_{ma} [M_{n^*}]^p \quad (14) \end{aligned}$$

For initiator:

$$\frac{1}{V_P} \frac{d}{dt} (V_P [I]^p) = 0 = 2K_i^p [I_2]^p - KP_i^p [I]^p [M]^p \quad (15)$$

$$\frac{1}{(V_0 - V_P)} \frac{d}{dt} \{ (V_0 - V_P) [I]^c \} = 0 = 2K_i^c [I_2]^c - KP_i^c [I]^c [M]^c \quad (16)$$

$$\frac{1}{V_P} \frac{d}{dt} (V_P [I_2]^p) = -K_i^p [I_2]^p - K_{ma} ([I_2]^c - [I_2]^p) \quad (17)$$

$$\frac{1}{(V_0 - V_P)} \frac{d}{dt} \{ (V_0 - V_P) [I_2]^c \} = -K_i^c [I_2]^c - K_{ma} ([I_2]^c - [I_2]^p) \quad (18)$$

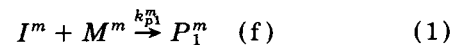
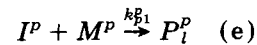
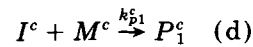
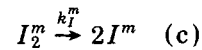
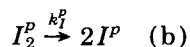
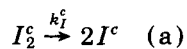
For monomer:

$$\frac{1}{V_P} \frac{d}{dt} (V_P [M]^p) = -K_P^p [I]^p [M]^p - K_P^p [M]^p \sum_{i=1}^{\infty} [P_i]^p - K_{trm}^p [M]^p \sum_{i=1}^{\infty} [P_i]^p - K_{ma} [M]^c - K_{ma} [M]^p \quad (19)$$

$$\frac{1}{(V_0 - V_P)} \frac{d}{dt} \{ (V_0 - V_P) [M]^c \} = -K_P^c [I]^c [M]^c - K_P^c [M]^c \sum_{i=1}^{\infty} [P_i]^c - K_{trm}^c [M]^c \sum_{i=1}^{\infty} [P_i]^c + K_{ma} ([M]^p - [M]^c) \quad (20)$$

3. Micelle phase formed by surfactant molecules (denoted by superscript m).

The initiator (I_2) and monomer (M) become distributed between these three phases and the concentrations of these in different phases need not be the same. The initiator molecules give primary radicals (I) through homolytic decomposition, which, in turn, combine with monomer to give polymer radicals as follows:



The polymer radicals add monomer molecules sequentially through a propagation reaction and grow in chain length. However, due to limited solubility of PMMA molecules in petrol, polymer molecules or radicals up to a critical chain length (say n^*) only stay in solution. Beyond this, it would undergo

Table II Moment Equations Derived from Results of Table I**Differential equations:**

$$\frac{1}{V_P} \frac{d}{dt} (V_P \lambda_{m0}^p) = K_i^p (\lambda_{p0}^p)^2 + K_{\text{trm}}^p [M]^p \lambda_{p0}^p \quad (1)$$

$$\frac{1}{V_P} \frac{d}{dt} (V_P \lambda_{m1}^p) = K_i^p \lambda_{p0}^p \lambda_{p1}^p + K_{\text{trm}}^p [M]^p \lambda_{p1}^p + K_{\text{trp}}^p \lambda_{m0}^p \lambda_{p1}^p - K_{\text{trp}}^p \lambda_{p0}^p \lambda_{m1}^p \quad (2)$$

$$\frac{1}{V_P} \frac{d}{dt} (V_P \lambda_{m2}^p) = K_i^p \lambda_{p0}^p \lambda_{p2}^p + K_{\text{trm}}^p [M]^p \lambda_{p2}^p + K_{\text{trp}}^p \lambda_{m0}^p \lambda_{p2}^p - K_{\text{trp}}^p \lambda_{p0}^p \lambda_{m2}^p \quad (3)$$

$$\frac{1}{(V_0 - V_P)} \frac{d}{dt} \{ (V_0 - V_P) \lambda_{m0}^c \} = K_i^c (\lambda_{p0}^c)^2 + K_{\text{trm}}^c [M]^c \lambda_{p0}^c \quad (4)$$

$$\frac{1}{(V_0 - V_P)} \frac{d}{dt} \{ (V_0 - V_P) \lambda_{m1}^c \} = K_i^c \lambda_{p0}^c \lambda_{p1}^c + K_{\text{trm}}^c [M]^c \lambda_{p1}^c + K_{\text{trp}}^c \lambda_{m0}^c \lambda_{p1}^c - K_{\text{trp}}^c \lambda_{p0}^c \lambda_{m1}^c \quad (5)$$

$$\frac{1}{V_0 - V_P} \frac{d}{dt} \{ (V_0 - V_P) \lambda_{m2}^c \} = K_i^c \lambda_{p0}^c \lambda_{p2}^c + K_{\text{trm}}^c [M]^c \lambda_{p2}^c + K_{\text{trp}}^c \lambda_{m0}^c \lambda_{p2}^c - K_{\text{trp}}^c \lambda_{m2}^c \lambda_{p0}^c \quad (6)$$

$$\frac{1}{V_P} \frac{d}{dt} (V_P \lambda_{p0}^p) = 0 = K_{p1}^p [M]^p [I]^p - K_i^p \lambda_{p0}^p + K_{\text{ma}}^c \lambda_{p0}^c - K_{\text{ma}}^p \lambda_{p0}^p \quad (7)$$

$$\begin{aligned} \frac{1}{V_P} \frac{d}{dt} (V_P \lambda_{p1}^p) = 0 = & K_{p1}^p [M]^p [I]^p - K_i^p \lambda_{p0}^p \lambda_{p1}^p + K_P^p [M]^p \lambda_{p0}^p \lambda_{p1}^p - K_{\text{trm}}^p [M]^p \lambda_{p0}^c \\ & - K_{\text{trm}}^p [M]^p \lambda_{p1}^c + K_{\text{trp}}^p \lambda_{p0}^p \lambda_{p1}^p - K_{\text{trp}}^p \lambda_{m0}^p \lambda_{p1}^p + K_{\text{ma}}^c \lambda_{p1}^c - K_{\text{ma}}^p \lambda_{p1}^p \end{aligned} \quad (8)$$

$$\begin{aligned} \frac{1}{V_P} \frac{d}{dt} (V_P \lambda_{p2}^p) = 0 = & K_{p1}^p [M]^p [I]^p - K_i^p \lambda_{p0}^p \lambda_{p2}^p + K_P^p [M]^p (2\lambda_{p1}^p + \lambda_{p0}^p) + K_{\text{trm}}^p [M]^p \lambda_{p0}^c \\ & - K_{\text{trm}}^p [M]^p \lambda_{p2}^c + K_{\text{trp}}^p \lambda_{p0}^p \lambda_{p2}^p - K_{\text{trp}}^p \lambda_{p2}^p \lambda_{m0}^p + K_{\text{ma}}^c \lambda_{p2}^c - K_{\text{ma}}^p \lambda_{p2}^p \end{aligned} \quad (9)$$

$$\frac{1}{(V_0 - V_P)} \frac{d}{dt} \{ (V_0 - V_P) \lambda_{p0}^c \} = K_i^c (\lambda_{p0}^c)^2 \lambda_{p1}^c + K_{P1}^c [M]^c [M]^c - K_{\text{ma}}^c \lambda_{p0}^c + K_{\text{ma}}^p \lambda_{p0}^p \quad (10)$$

$$\begin{aligned} \frac{1}{(V_0 - V_P)} \frac{d}{dt} \{ (V_0 - V_P) \lambda_{p1}^c \} = & K_i^c \lambda_{p0}^c \lambda_{p1}^c + K_{P1}^c [I]^c [M]^c + K_P^c [M]^c \lambda_{p0}^c \\ & + K_{\text{trp}}^c \lambda_{m1}^c \lambda_{p0}^c - K_{\text{trp}}^c \lambda_{m0}^c \lambda_{p1}^c + k_{\text{trm}}^c \lambda_{p0}^c [M]^c - K_{\text{ma}}^c \lambda_{p1}^c + K_{\text{ma}}^p \lambda_{p1}^p \end{aligned} \quad (11)$$

$$\begin{aligned} \frac{1}{(V_0 - V_P)} \frac{d}{dt} \{ (V_0 - V_P) \lambda_{p2}^c \} = & K_i^c \lambda_{p0}^c \lambda_{p2}^c + K_{P1}^c [I]^c [M]^c + K_P^c [M]^c (2\lambda_{p1}^c - \lambda_{p0}^c) \\ & + K_{\text{trp}}^c \lambda_{m2}^c \lambda_{p0}^c - K_{\text{trp}}^c \lambda_{p2}^c \lambda_{m0}^c + k_{\text{trm}}^c \lambda_{p0}^c [M]^c - k_{\text{trm}}^c [M]^c \lambda_{p2}^c - K_{\text{ma}}^c \lambda_{p2}^c + K_{\text{ma}}^p \lambda_{p2}^p \end{aligned} \quad (12)$$

Algebraic equations for all intermediate species:

$$K_{p1}^p [M]^p [I]^p - K_i^p \lambda_{p0}^p + K_{\text{ma}}^c (\lambda_{p0}^c - \lambda_{p0}^p) = 0 \quad (13)$$

$$\begin{aligned} K_{p1}^p [M]^p [I]^p + K_P^p [M]^p \lambda_{p0}^p - K_i^p \lambda_{p0}^p \lambda_{p1}^p + K_{\text{trm}}^p [M]^p \lambda_{p0}^p + K_{\text{trp}}^p \lambda_{m1}^p \lambda_{p0}^p \\ - K_{\text{trm}}^p [M]^p [\lambda_{p1}]^p - K_{\text{trp}}^p \lambda_{m0}^p \lambda_{p1}^p + K_{\text{ma}}^c (\lambda_{p1}^c - \lambda_{p1}^p) = 0 \end{aligned} \quad (14)$$

Table II (Continued)

Algebraic equations for all intermediate species:

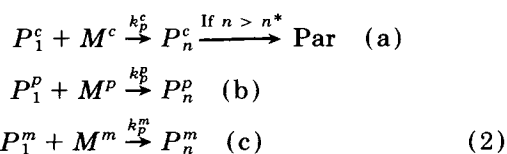
$$K_{p1}^p[M]^p[I]^p + K_p^p[M]^p(2\lambda_{p1}^p + \lambda_{p0}^p) - K_t^p\lambda_{p0}^p\lambda_{p2}^p + K_{trm}^p[M]^p\lambda_{p0}^p - K_{trm}^p[M]^p\lambda_{p2}^p + K_{trp}^p\lambda_{p0}^p\lambda_{m2}^p - K_{trp}^p\lambda_{p2}^p\lambda_{m0}^p + K_{ma}(\lambda_{p2}^c - \lambda_{p2}^p) = 0 \quad (15)$$

$$- K_t^c + K_{p1}^c[I]^c[M]^c - K_{ma}(\lambda_{p0}^c - \lambda_{p0}^p) = 0 \quad (16)$$

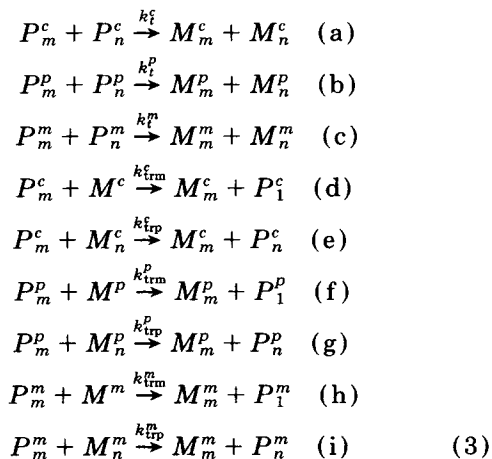
$$K_{p1}^c[I]^c[M]^c - K_t^c\lambda_{p0}^c\lambda_{p1}^c + K_p^c[M]^c\lambda_{p0}^c + K_{trp}^c\lambda_{m1}^c\lambda_{p0}^c - K_{trp}^c\lambda_{m0}^c\lambda_{p1}^c + K_{trm}^c[M]^c\lambda_{p0}^c - K_{trm}^c\lambda_{p1}^c[M]^c + K_{ma}(\lambda_{p1}^c - \lambda_{p0}^p) = 0 \quad (17)$$

$$K_{p1}^c[I]^c[M]^c - K_t^c\lambda_{p0}^c\lambda_{p2}^c + K_p^c[M]^c(2\lambda_{p1}^c + \lambda_{p0}^p) + K_{trp}^c\lambda_{m2}^c\lambda_{p0}^c - K_{trp}^c\lambda_{p2}^c\lambda_{m0}^c + K_{trm}^c[M]^c\lambda_{p0}^c - K_{trm}^c[M]^c\lambda_{p2}^c + K_{ma}(\lambda_{p2}^c - \lambda_{p2}^p) = 0 \quad (18)$$

homogeneous nucleation to form a new particle as follows:

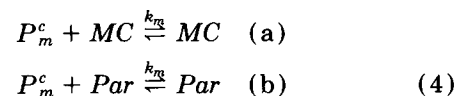


Above in eq. 2(a), Par represents a polymer particle. Polymer radicals P_n of MMA under transfer and disproportionation-type termination reactions to form dead polymer chains (M_n , where n is the chain length). The transfer reaction could occur either by monomer or dead polymer molecules as

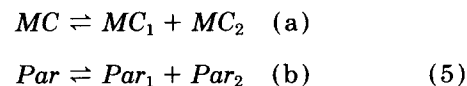


Various polymerization reactions have now been accounted for in eqs. (1)–(3), and from these, it appears that different phases undergo chemical reactions independent of each other. In fact, polymer radical growing in petrol phase [through eq. (2a)]

can be absorbed by particle or micelle phases much before homogeneous nucleation. In addition, the particle and micelle (MC) phases can desorb polymer radicals and the absorption–desorption process could be represented by



Besides this, two polymer particles or micelles, MC, can undergo coalescence or breakage as



As the polymerization progresses, the volume fraction of the particle phase (Par) increases. In addition to this, concentrations of various species need not be the same. Instead of addressing the most general problem, we assume that it is possible to define some average concentration that is the same for all particles. If we define all polymer particles put together as one system having volume V_p , then this is changing with time due to formation of polymer that is occurring continuously. We can make a mole balance after observing that the coagulation of particles, as in Eq. (5), do not contribute anything to the mole balance relations. These are given in Table I. There are several occasions when we wish to know the moments of distributions only. We observe that we have two different distributions for polymer radicals, P_n , and dead polymer chains, M_n , and as a consequence, we have the following three moments:

$$\lambda_{mi}^p = \sum_{n=2}^{\infty} n^i [M_n^p]; \quad i = 0, 1, 2 \quad (\text{a})$$

$$\lambda_{mi}^c = \sum_{n=2}^{\infty} n^i [M_n^c]; \quad i = 0, 1, 2 \quad (\text{b})$$

$$\lambda_{mi}^m = \sum_{n=2}^{\infty} n^i [M_n^m]; \quad i = 0, 1, 2 \quad (\text{c})$$

$$\lambda_{pi}^p = \sum_{n=1}^{\infty} n^i [P_n^p]; \quad i = 0, 1, 2 \quad (\text{d})$$

$$\lambda_{pi}^c = \sum_{n=1}^{\infty} n^i [P_n^c]; \quad i = 0, 1, 2 \quad (\text{e})$$

$$\lambda_{mi}^m = \sum_{n=1}^{\infty} n^i [P_n^m]; \quad i = 0, 1, 2 \quad (\text{f}) \quad (6)$$

The expressions for these can be easily derived from relations given in Table I and these have been summarized in Table II.

The mole balance and moment equations consist of differential as well as algebraic equations. The differential equations have been solved by the fourth-order Runge-Kutta technique. The algebraic equations are solved calling a subroutine RADICAL, where the sequential computations for the zeroth, first, and second moments of the polymer radical species in both phases have been carried out. After proper elimination, a quartic equation in λ_{p0}^c has been obtained which has been solved by Newton-Raphson technique. The time increment in Runge-Kutta was kept at 20 s and computations were carried out for a total time span of 6000 s of dispersion polymerization.

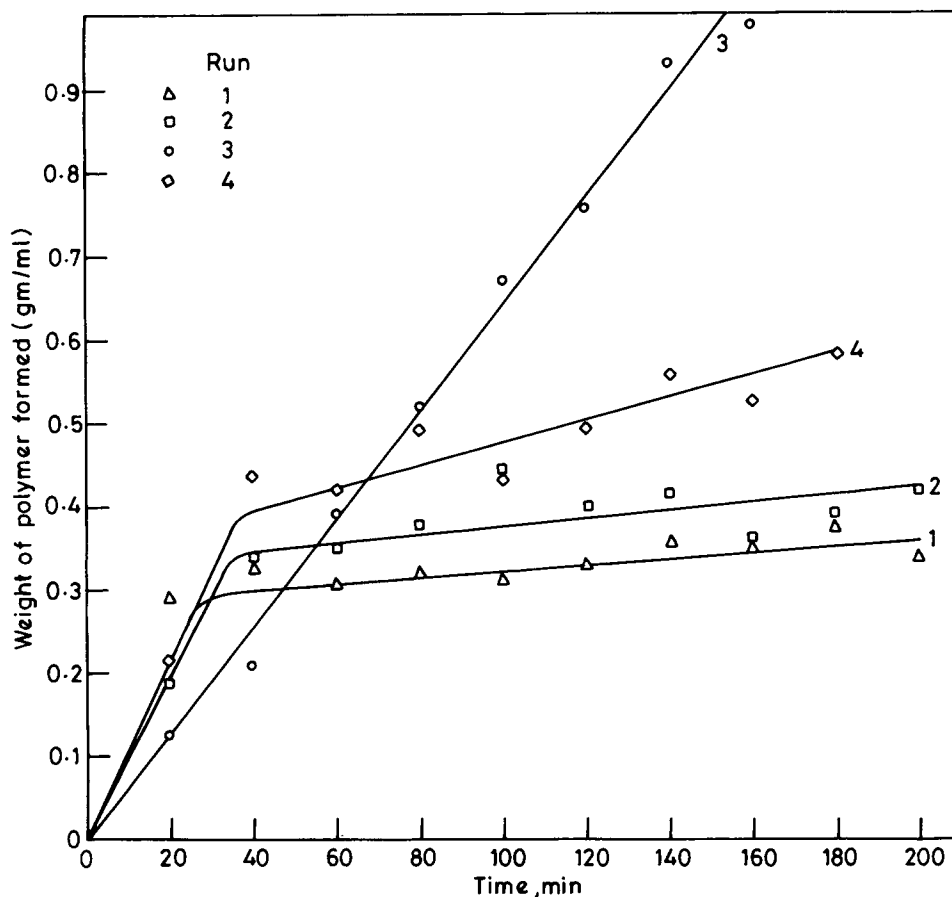
RESULTS AND DISCUSSION

To carry out the dispersion polymerization of MMA in petrol, we prepared the graft-comb stabilizer as described in Appendix I. The selection of the reaction medium is extremely crucial for carrying out the dispersion polymerization. The reason why we chose petrol was because it is relatively cheap and has high vapor pressure, which would give quick drying. The petrol used in our studies has been completely characterized in Appendix II. It may be recalled that the solubility characteristics of petrol lies somewhere between those of heptane and toluene. We have carried out experiments in both these mediums and we find that dispersion polymerization does not occur in either of these.

After the successful preparation of the stabilizer copolymer in Appendix I, we carried out a systematic study of dispersion polymerization. We prepared the copolymer with different chain lengths n , of the grafts of poly(1,2-hydroxystearic acid). The case of $n = 1$ corresponds to the endcapping of 12-hydroxystearic acid monomer, and we find that the stabilizer copolymer for this case does not give the dispersion polymerization of MMA in petrol. For all possible concentration ranges of this stabilizer, the PMMA coagulated and separated into different layers within 20 min of polymerization. However, the stabilizer copolymer having $n = 2-4$ gave an excellent dispersion of PMMA in petrol. We carried out the experimental study of dispersion polymerization and measured the amount of PMMA formed and its molecular weight as a function of time.

We have systematically varied the amount of stabilizer copolymer used and the experimental results of the rate, and molecular weight for different runs are given in Figures 3-6. In Figures 3 and 4, results for rate and molecular weight show that there is a transition region for about 50 min and then the rate takes on a steady value, whereas the molecular weight takes on an asymptotic level. A similar effect has been obtained in Figures 5 and 6 when the chain length of the branches of the stabilizer copolymer is increased from $n = 2$ to $n = 4$. The only difference lies for $n = 4$ in that it takes about 100 min. We have tested the dispersion polymerization with AIBN as well as with a benzoyl peroxide initiator and we find that for a given initiator concentration the rate of polymer formation is lower for the benzoyl peroxide. This can be explained by the fact that this initiator has a lower rate constant of dissociation and, as a consequence, at any given time, there are fewer growing polymer radicals in the reaction mass.

The rate data in Figures 3 and 5 for $n = 2$ and 4 needs careful examination. After the steady state is reached, we find that the rate for $n = 2$ depends on the concentration of the stabilizer copolymer used, as opposed to this for $n = 4$, which is not found to be the case. This can be discerned from Figure 5 by the constant slope of lines even though the polymer content of the reaction mass for various runs are different. If the polymer content of the reaction mass at a given time is compared between these two figures, it is observed that the stabilizer of $n = 4$ is at least three times more effective. In the runs of Figure 4, the amount of stabilizer copolymer used is about three times more compared to that used in Figure 6 even though the amount of polymer formed is comparable.



	Run 1		Run 2		Run 3		Run 4	
	Seed	Feed	Seed	Feed	Seed	Feed	Seed	Feed
AIBN	4.790	0.2324	4.790	0.2324	4.790	0.2324	4.790	0.2324
MMA	9.952	109.0900	9.952	109.0900	9.952	109.0900	9.952	109.0900
MA	0.133	2.2620	0.133	2.2620	0.133	2.2620	0.133	2.2620
Petrol	300	—	300	—	300	—	300	—
Dispersion (solid content)	—	10 (3.25)	—	15 (4.87)	—	5 (1.63)	—	20 (6.50)

AIBN: azobisisobutyronitrile; MMA: methyl methacrylate; MA: methacrylic acid.

Figure 3 Weight of polymer formed with time in dispersion polymerization of MMA in petrol using surfactant having $n = 2$.

From Figures 4 and 6, we find the molecular weight of the polymer formed is greatly affected by the amount of stabilizer used. For a specified chain length of the branches of the copolymer, we find that as the concentration is increased the molecular weight of the PMMA increases. However, beyond a certain value, the molecular weight reduces and this phenomena can be explained as follows: When we

add the stabilizer to the reaction mass, it does not go into the solution completely. As explained earlier, the backbone chains are compatible with PMMA. In petrol medium, these stabilizer molecules exist in the form of micelles and they constitute the loci for polymerization of MMA. The monomer diffuses from the petrol phase into it and grow in chain length therein. As the concentration of the stabilizer

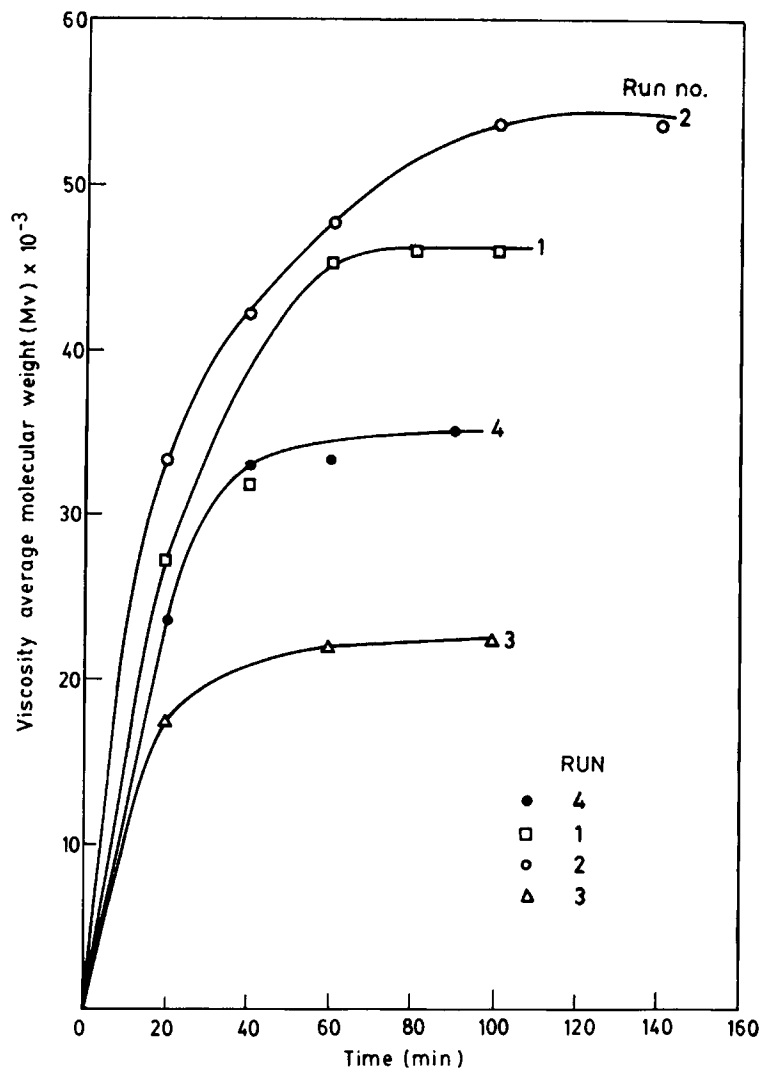
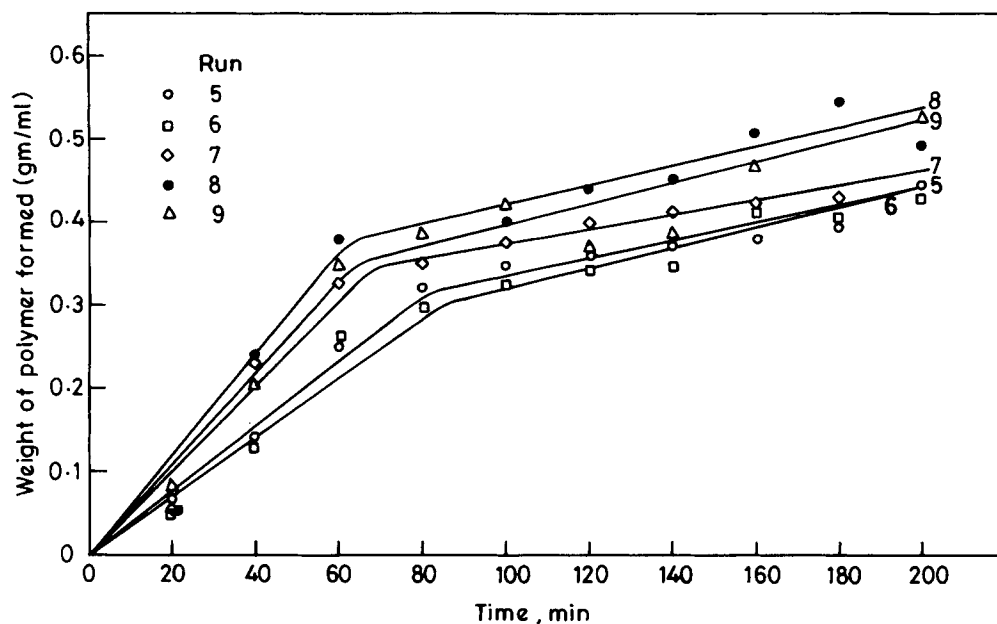


Figure 4 Viscosity-average molecular weight of the polymer in dispersion polymerization of MMA in petrol with surfactant having branch chain length $n = 2$.

increases, it is expected that the number of such sites increases and this would lead to higher rate and larger molecular weight of the PMMA. As opposed to this, when the concentration of the stabilizer is increased beyond a certain value, the domains of micelles begin to interact with each other. When this interaction increases, the surfactant chains begin to become entangled with each other, this way serving as a barrier to the diffusion of the monomer. As a result of the reduced monomer diffusion, the rate as well as the molecular weight of the final polymer are expected to fall, which is what has been observed in Figures 4 and 6.

The dispersion polymerization of MMA in petrol gives a heterogeneous reaction medium. It has a

PMMA phase dispersed in the petrol medium. The initiator AIBN or benzoyl peroxide is expected to be distributed in both the phases as it dissolves in them. However, their actual concentration will depend on the dissolution thermodynamics. The mole balance relations for various reaction species have been derived earlier. It is observed that both the volume and the concentration of various species change with time, but earlier studies on heterogeneous polymerization as in emulsion polymerization have shown that the polymer formation could always be divided into two clear-cut time domains. In the first stage, the volume changes are small, whereas the concentration changes are relatively fast. As opposed to this, in the second stage, the concentrations



	Run 5		Run 6		Run 7		Run 8		Run 9	
	Seed	Feed	Seed	Feed	Seed	Feed	Seed	Feed	Seed	Feed
BP	4.790	0.2324	4.790	0.2324	4.790	0.2324	4.790	0.2324	4.790	0.2324
MMA	9.952	109.1600	9.952	109.1600	9.952	109.1600	9.952	109.1600	9.952	109.1600
MA	0.133	2.2620	0.133	2.2620	0.133	2.2620	0.133	2.2620	0.133	2.2620
Petrol	300	—	300	—	300	—	300	—	300	—
Dispersion (solid content)	—	31.6 (3.25)	—	47.39 (4.876)	—	15.79 (1.625)	—	10.37 (1.067)	—	20.2700 (2.0860)

BP: benzoyl peroxide.

Figure 5 Weight of polymer formed with time in dispersion polymerization of MMA in petrol using surfactant with branch chain length $n = 4$.

do not change and the polymerization leads to the growth of the polymer phase only.

In deriving the moment equations in Table II, we have assumed that all molecular species can diffuse from the continuous phase of petrol to the polymer phase. This may be understood that through homogeneous nucleation all molecular species having chain length of more than n^* become transferred to the polymer phase. This fact can be modeled mathematically and has been shown in Table II. The moment equations are seen not to involve n^* , which is because we have ignored the homogeneous nucleation. If we wish to accommodate this, then the moment equations are different and as an illustration in the following, we derive the relation for the zeroth moment, λ_{p0} :

$$-k_t^c (\lambda_{p0}^c)^2 + k_p^c [I]^c [M]^c + k_m a \left(\sum_{n=1}^{n^*} [P_n^c] - \lambda_{p0}^c \right) = 0$$

$$-k_t^p (\lambda_{p0}^c)^2 + k_p^p [I]^p [M]^p - k_m a \left(\sum_{n=1}^{n^*} [P_n^p] - \lambda_{p0}^c \right) = 0$$

Pohlein et al.²⁸ discussed the value of n^* for various systems, and for MMA, n^* is reported to be 66 in water. As a consequence, we have assumed for petrol medium that

$$\sum_{n=1}^{n^*} [P_n] \approx \sum_{n=1}^{\infty} [P_n]^c = \lambda_{p0}^c$$

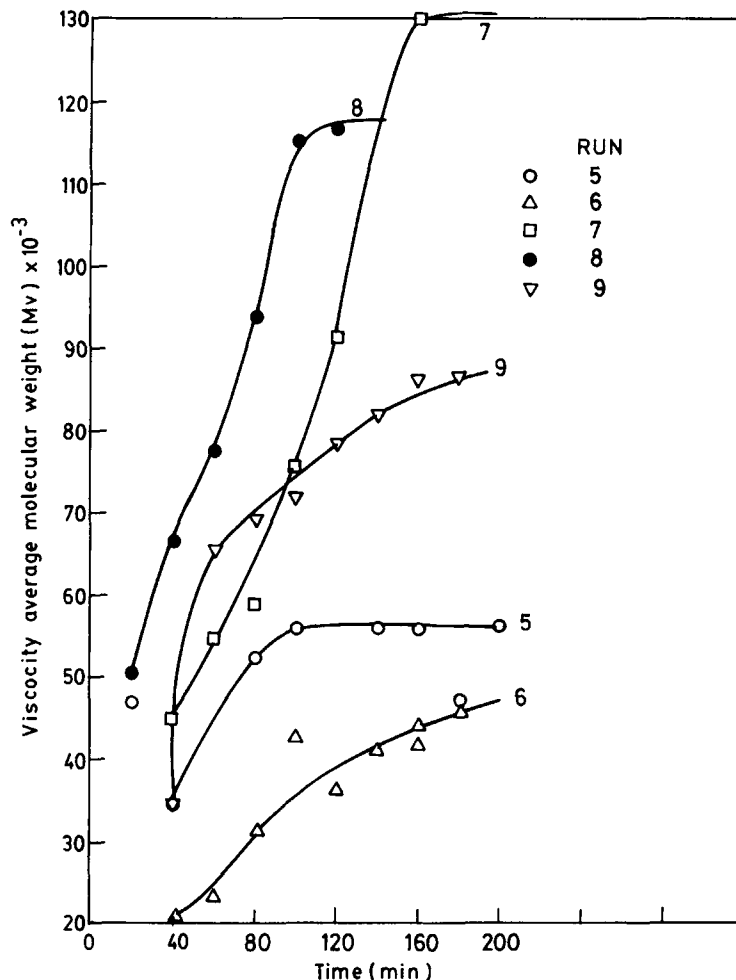


Figure 6 Viscosity-average molecular weight of polymer formed in dispersion polymerization of MMA in petrol using surfactant with branch chain length $n = 4$.

Under this case, the moment equations of Table III can be taken as a good representation of the dispersion polymerization of MMA in petrol.

We have simulated the set of algebraic and differential equations of Table II on a PC-XT computer. The algebraic equations have been arranged in such a way that sequential computations of various radical species could be carried out. If proper eliminations are carried out, we obtained a quartic equation in λ_{p0}^c . Instead of solving this analytically, we decided to use the Newton-Raphson technique in which their values in the previous step was used as the present guess. This technique was found to be extremely efficient and the solution converges within a maximum of five trials. The differential equations governing the concentration of stable species were solved using the fourth-order Runge-Kutta technique. The computation of the reactor performance was extremely efficient, and stable nu-

merical results could be generated for a given set of rate constants.

To evaluate the relative effect of various reactor parameters, we varied them systematically and results are reported in Figures 7-11. In Figure 7, we varied the propagation rate constants and reported the average chain length of the polymer as a function of reaction time. For a small values of the rate constant, we find the molecular weight rises first and then reaches an asymptotic value. However, when the k_p is increased beyond the value of 2000, the molecular weight is found to reduce after having undergone a maximum. This can be explained by observing that in the polymer phase the monomer is depleted through polymerization and is replenished through diffusion from the continuous phase. When the rate of polymerization is large, the monomer concentration within the polymer phase is reduced, giving a lower molecular weight as observed in Figure

Table III Various Rate Constants Chosen to Fit the Experimental Data (All Second-Order Rate Constants are in L mol/s)

Rate Constants	Run No.								
	1	2	3	4	5	6	7	8	9
$k_m \times 10^{-4}$	8.500	1.800	0.950	0.170	0.330	0.060	0.255	0.120	0.000
$k_p^p \times 10^{-4}$	0.006	0.006	0.006	0.006	0.150	0.150	0.150	0.150	0.000
$k_i^i \times 10^{-4}$	0.006	0.006	0.006	0.006	0.150	0.150	0.150	0.150	0.000
$k_{pi}^p = k_p^p$	350.000	350.000	350.000	100.000	1000.000	1000.000	1000.000	1000.000	10.000
$k_{pi}^c = k_p^c$	300.000	300.000	300.000	50.000	573.000	573.000	573.000	573.000	5.000
$k_t^p \times 10^{-6}$	50.000	50.000	90.000	90.000	87.000	87.000	87.000	87.000	0.0
$k_t^c \times 10^{-6}$	65.000	65.000	95.000	95.000	80.000	80.000	80.000	80.000	0.0
k_{trm}^p	0.138	0.138	0.138	0.138	0.138	0.138	0.138	0.138	0.000
k_{trm}^c	0.138	0.138	0.138	0.138	0.138	0.138	0.138	0.138	0.000
k_{trp}^p	0.150	0.150	0.150	0.150	0.150	0.150	0.150	0.150	0.000
k_{trp}^c	0.150	0.150	0.150	0.150	0.150	0.150	0.150	0.150	0.000

7. For small k_p , the rate of diffusion is sufficient to maintain the dynamic equilibrium between the two phases, and as a result of that, an asymptotic molecular weight is obtained. In addition to this, increasing k_p leads to higher molecular weight, as seen from Figure 7. A similar effect is obtained when we

varied the termination rate constant in Figure 8. As we increase k_t , the lifetime of a polymer radical is reduced, and as a result, the molecular weight is found to fall. On reducing k_t , the rate of polymerization increases, and as a result of this, the average chain length of the polymer begins to fall after

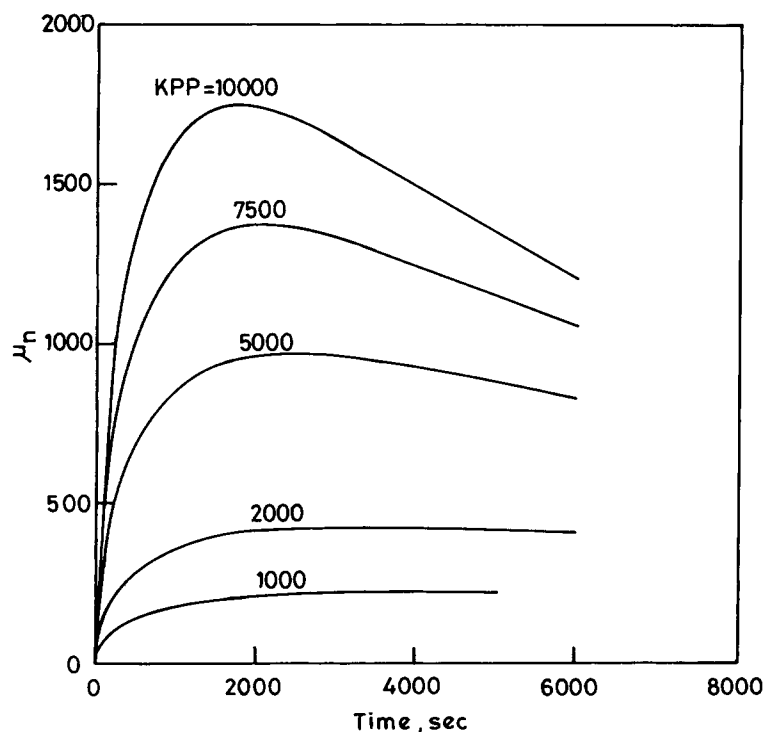


Figure 7 Effect of k_p upon μ_w of polymer formed. Base rate constant values are $k_p^c = 573$, $k_p^p = 1000$, $k_t^p = 50 \times 10^6$, $k_t^c = 50 \times 10^6$, $k_m = 0.004$, $k_{trm}^p = k_{trm}^c = 0.138$, $k_{trp}^c = k_{trp}^p = 0.15$, and $k_i^p = k_i^c = 0.15 \times 10^{-4}$.

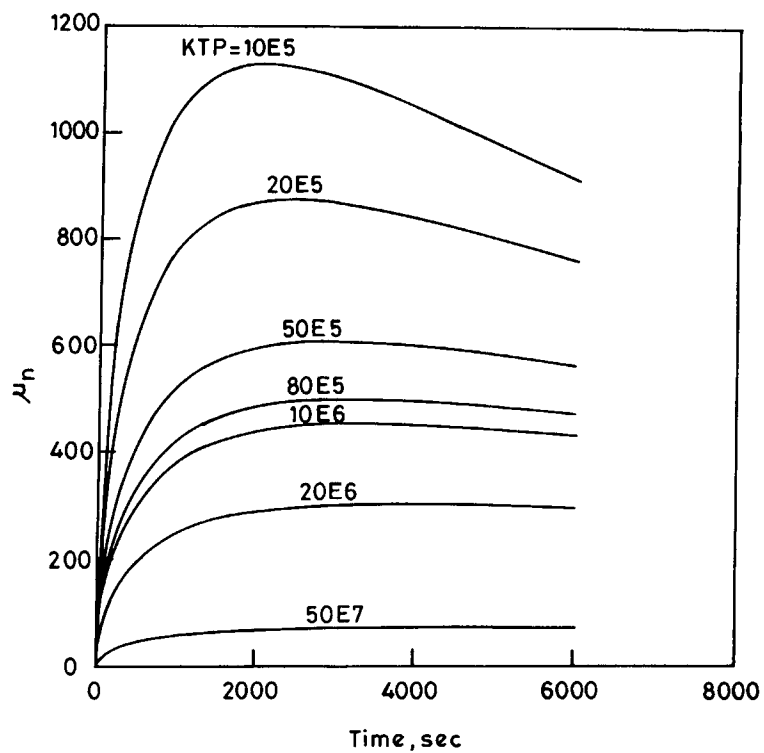


Figure 8 Effect of k_t upon μ_w of polymer formed. Base rate constant values are given in Figure 7.

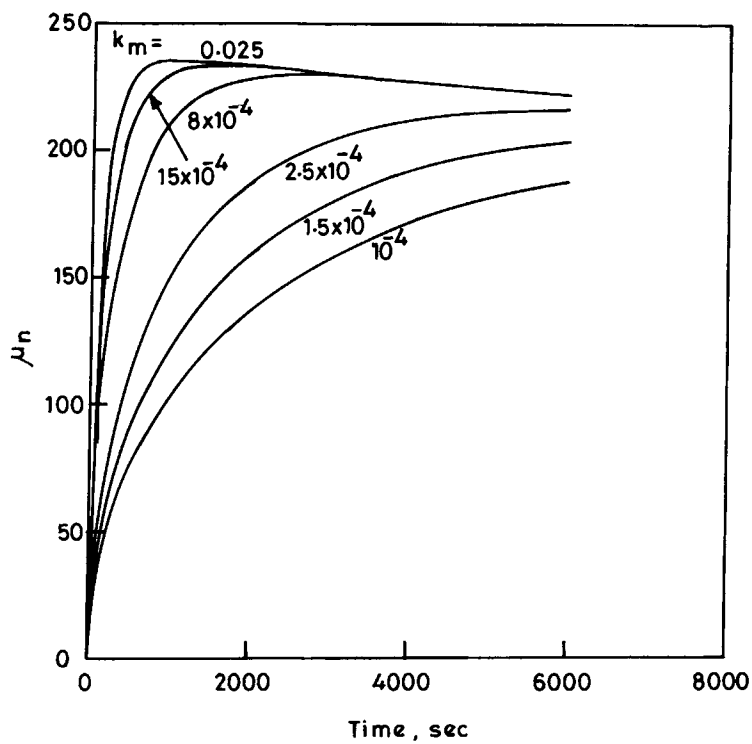


Figure 9 Effect of k_m upon μ_w of polymer formed. Base rate constant values are given in Figure 7.

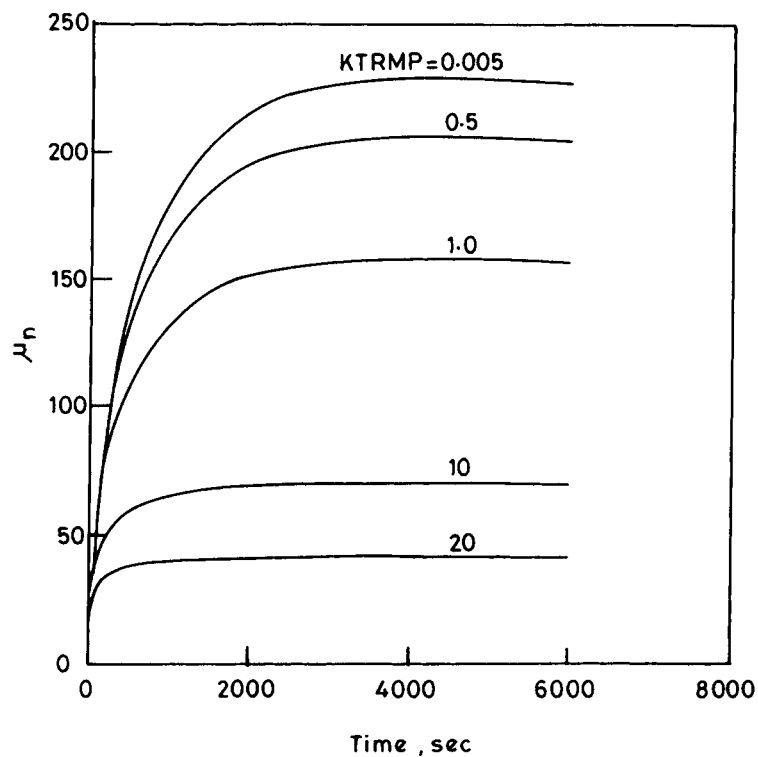


Figure 10 Effect of k_{trm}^p upon μ_w . Base rate constant values are given in Figure 7.

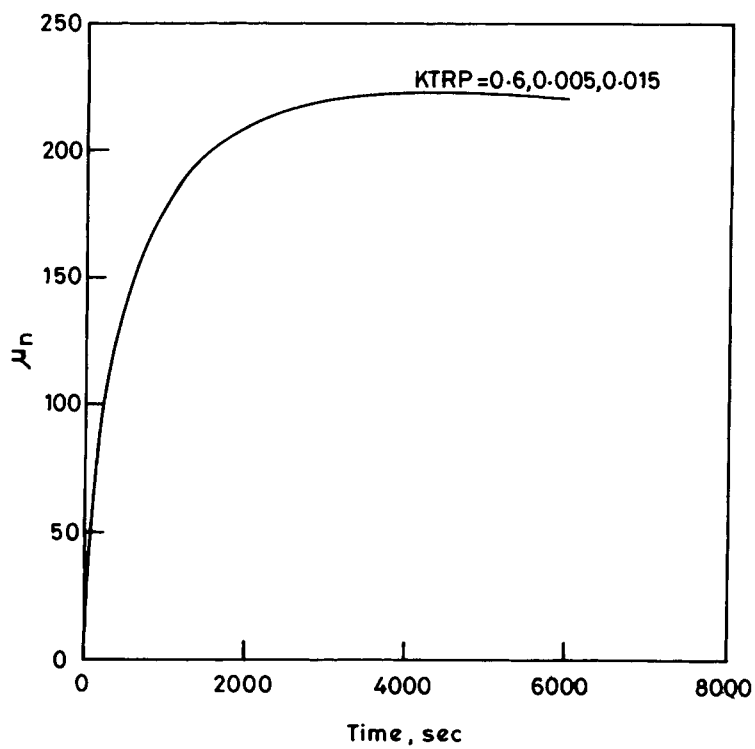


Figure 11 Effect of k_{trp}^p upon μ_w . Base rate constant values are given in Figure 7.

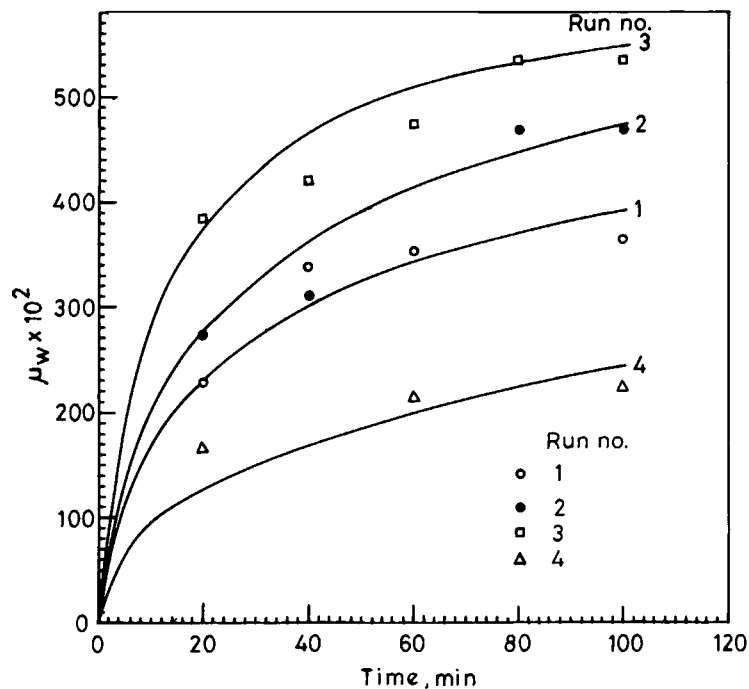


Figure 12 Curve fitting of experimental data of Figure 4.

reaching a maximum value, due to the reduction in the monomer concentration within that phase.

In Figure 9, we examined the variation of the monomer diffusivity. We noticed that as we reduce

the value of K_m the time taken to reach the second stage of polymerization is increased. From our experimental data of Figures 4 and 6 on molecular weight as a function of time, we can easily determine

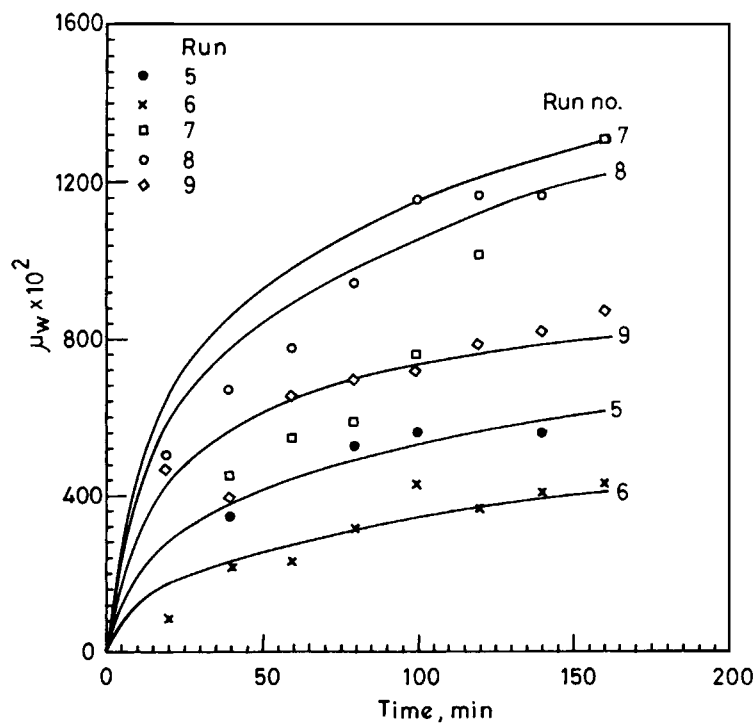


Figure 13 Curve fitting of experimental data of Figure 6.

the induction time, and from this figure, we can evaluate the value of k_m very conveniently. We have generated Figure 10 by varying the transfer rate constant to monomer, k_{tm}^p . We find that as we increase the value of this, the asymptotic average chain length of the polymer falls, as is expected. In Figure 11, we examined the effect of variation of the transfer rate constant to the polymer, k_{tp}^p , and find that there is no effect upon the course of polymerization for a wide variation of this rate constant. Lastly, we attempted to use the kinetic model to fit the experimental data. We have found the rate constants by trial-and-error, which predicts the experimental molecular weight of PMMA in the entire time domain. The simulated curves and experimental points are given Figures 12 and 13. The assumed rate constants have been summarized in Table III. The value of k_m is essentially decided by the total time of transience, and the termination rate constants k_t , by the asymptotic level of the molecular weight of PMMA. In all these simulations, we have assumed that the propagation rate constants are essentially invariant. This is done because k_p involves the reaction between M and the polymer radicals and is not expected to vary because of the ASB effects discussed earlier.

CONCLUSION

To carry out dispersion polymerization in the non-aqueous phase, petrol, we need a special stabilizer copolymer. In this work, we synthesized a comb copolymer with the pendant segments groups of poly(Hydroxystearic acid) and the backbone of PMMA. We find that if the stabilizer copolymer precipitates from the solution it can never be dissolved again. In this work, we systematically varied the chain length of the branches of poly(hydroxystearic acid) and found that this has great effect on the course of polymerization. For example, for the chain length of $n = 1$, there is no stabilizing effect, whereas for $n = 4$, we obtain the best results, in terms of the rate as well as the molecular weight of the polymer formed.

The polymerization of MMA occurs in two phases, viz., the continuous phase of petrol with PMMA particles dispersed in it. When the dispersion polymerization is initiated, the stabilizer copolymer is present in the petrol phase in the form of micelles. To sustain the polymerization, the monomer has to diffuse from the petrol to these micelles. As the concentration of the micelles increases, the number of micelles first increases, but for large

concentrations, their domains begin to interact with each other. When the number increases, the rate as well as the molecular weight are found to be increased. However, when the interaction between them starts, the chains begin to be held tightly, which adversely affects the diffusion of monomer in it. This is found to give a fall in the molecular weight of the polymer formed. Our experimental results show exactly this and we have found that there is an optimal concentration of the surfactant for given chain length of the pendant poly(hydroxystearic acid) of the stabilizer copolymer.

The two-phase dispersion polymerization has been modeled mathematically in this work. We have divided the reaction mass into the polymer and the continuous phases and have written down the mole balance relations of various species for both these phases. Earlier work on emulsion polymerization showed that the polymerization can be divided into two stages, where in the first stage the change in the concentration of the species occurs. As opposed to this, in the second stage, the concentrations are essentially time invariant and the polymerization leads to the growth of the particles. The solution of the differential equations can be conveniently implemented on a personal computer and the computer results can be found to confirm with the experimental findings. We shown that it is possible to curve-fit the experimental molecular weight data. We have determined the set of rate constants that describe them in the entire range.

The authors wish to thank the Department of Science and Technology, New Delhi, India, for partial financial support.

APPENDIX I

Procedure of Preparing PMMA Grafted-Poly(12-hydroxystearic acid) Copolymer of Controlled Graft Length

The preparation of the copolymer stabilizer having a controlled graft length requires several steps, which are given below:

Step 1: Preparation of poly(12-hydroxy-stearic acid) of desired chain length:

12-Hydroxy stearic acid of a measured amount was added to the reactor at 180°C. (Beyond this temperature, there is sufficient charring of the polymer.) Before applying the vacuum, the reactor was first purged with argon for 15–30 min. The reactor was then connected to a vacuum pump to obtain about a 25 mmHg vacuum. One to two

grams of the sample was withdrawn at regular intervals for measuring the conversion. It was dissolved in 100 mL dimethylformamide (DMF) and filtered. The resultant clear solution was then titrated to obtain the conversion of the functional group as follows. A sodium hydroxide solution of standard $N/10$ concentration was used for the titration with 0.3% Thymol blue solution in methanol as the indicator.

The polymerization of 12-hydroxystearic acid at 180°C proceeds up to approximately 40% conversion on its own, but for values beyond this, we need to apply high vacuum. To obtain the chain length of about four, we must obtain 75% conversion of the functional group. This required the polymerization time of about 4 days under the vacuum of 25 mmHg. The resultant polymer is light brown in color, having the appearance of grease.

Step 2 Reaction of glycidyl methacrylate to poly(12-hydroxystearic acid) in presence of amine catalyst.

The reaction was carried out in the same experimental setup as earlier without a vacuum at a temperature of $165 \pm 0.1^{\circ}\text{C}$. The terminal carboxyl groups of the polyester are converted to methacrylate residues by this reaction using 1.5 molar excess of glycidyl methacrylate in the presence of amine catalyst. The relative amount of glycidyl methacrylate depends upon the chain length of the poly(12-hydroxystearic acid) used. After the temperature was attained, the feed mixture [weight ratio: poly(hydroxystearic acid) (47.02), glycidyl methacrylate, triethanol amine (0.09), hydroquinone (0.05), xylene (47)] was introduced. Triethanol amine was used as the catalyst and hydroquinone was added to stop further reaction.

For kinetic studies, the product was withdrawn using a pipette after a time interval of 15–30 min in a 25 mL beaker of known weight. The sample was dissolved into 50 mL DMF and was then titrated against the sodium

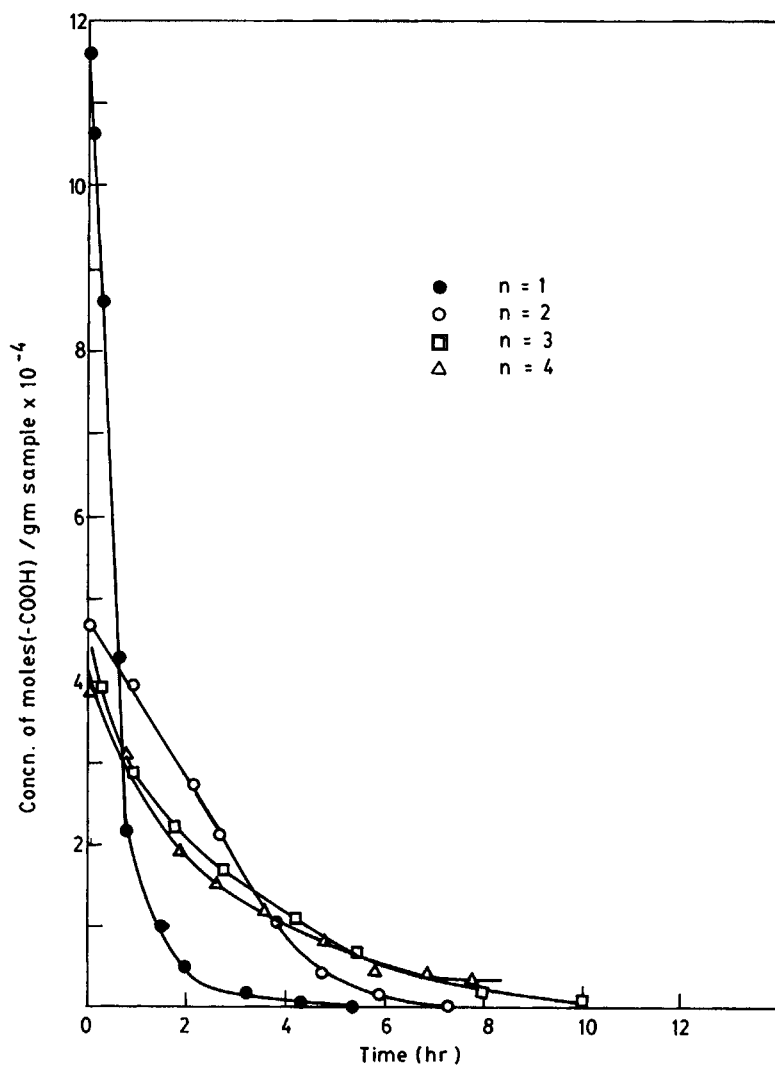


Figure A.1 Concentration of [COOH] groups vs. time.

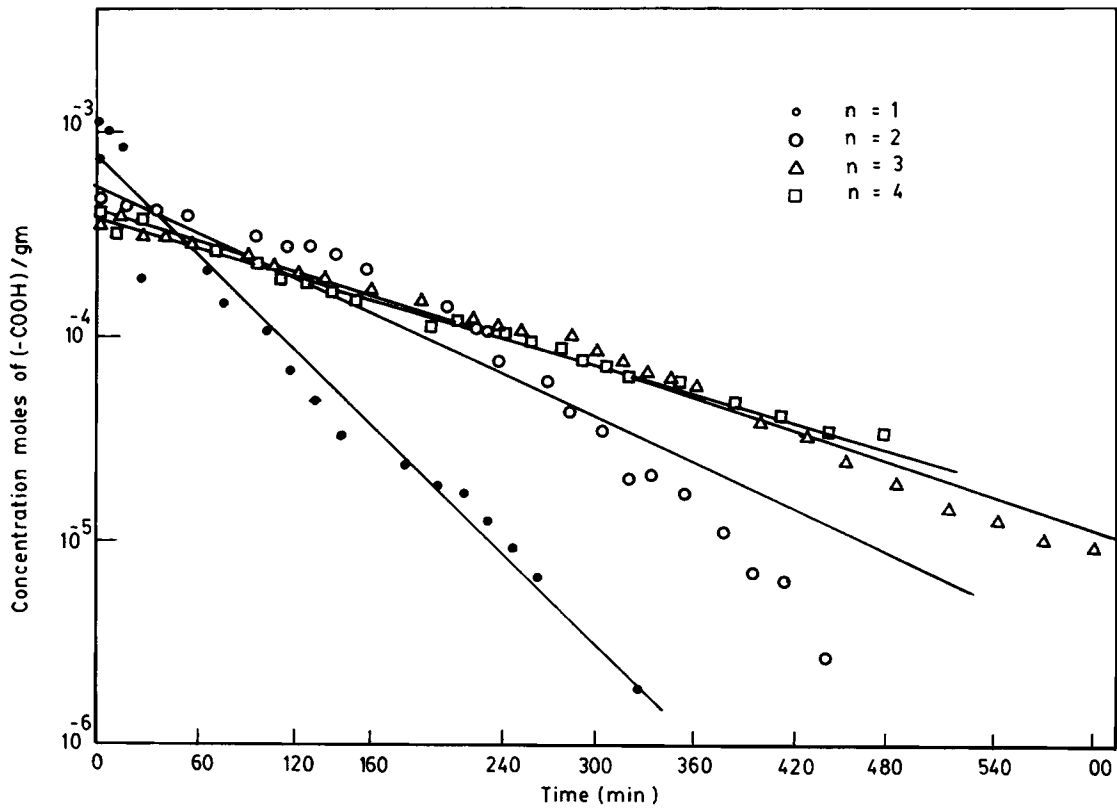


Figure A.2 First-order plot of [COOH] concentration vs. time.

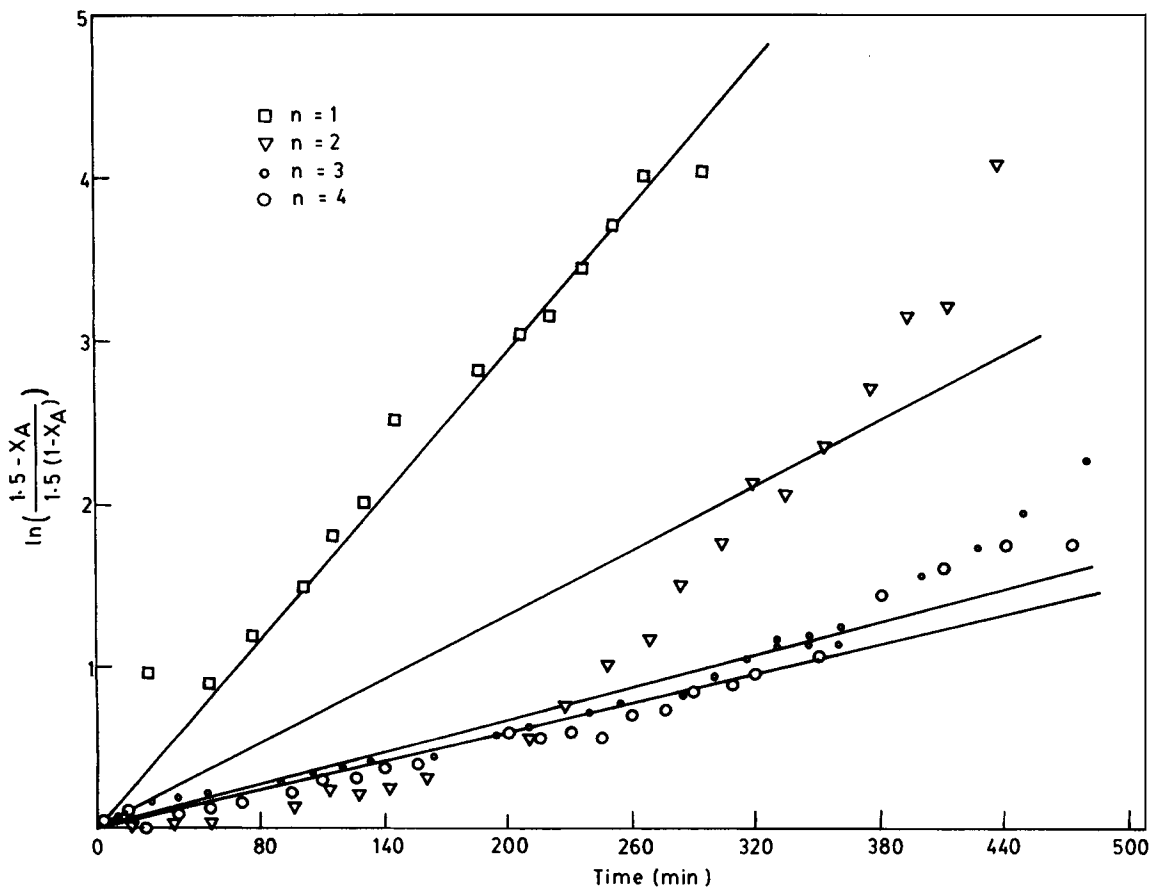


Figure A.3 Second-order plot of [COOH] concentration with time.

Table A.I Values of Rate Constants Obtained from First-Order Plot for Different Chain Lengths n of Poly(hydroxystearic Acid)

n	$(k \text{ min}^{-1}) \times 10^{-3}$
1	7.95
2	3.76
3	2.42
4	2.29

methacrylate solution in a benzene-methanol mixture to measure the concentration of the $-\text{COOH}$ group. The reaction was continued until the acid content of 1 g of sample reached about 2×10^{-6} mol. The course of polymerization is presented in Figure A.1. We first correlated the experimental rate data by the following first-order reaction expression involving the acid groups on the polymer chains:

$$\frac{d}{dt} [\text{COOH}] = -k[\text{COOH}]$$

In this equation, $[\text{COOH}]$ represents the concentration of the acid functional group in mol/g of the sample. The results have been plotted on a semilog scale in Figure A.2

and we find that the experimental data can be correlated well by a straight line in a semilog plot. The examination of this figure shows clearly the effect of chain length on the rate of reaction of glycidyl methacrylate. We noticed that the endcapping rate is considerably fast for $n = 1$ compared to that for $n = 4$. Results for $n = 3$ and $n = 4$ are very close and indistinguishable from the experimental errors. From Figure A.3, we calculated the slope of various straight lines and reported the first-order rate constants in Table A.I. We notice that the rate constant falls from the value of $7.95 \times 10^{-3}/\text{min}$ for $n = 1$ to $2.3 \times 10^{-3}/\text{min}$ for $n = 4$, a value that appears to be independent of chain length.

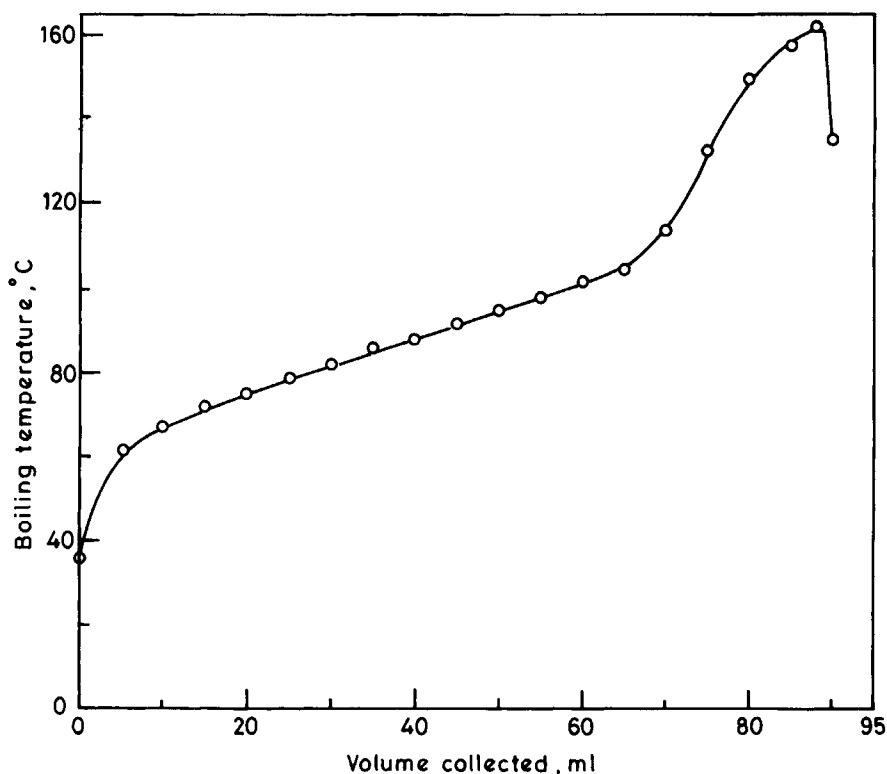
In Figure A.3 we examined the following second-order plot:

$$\frac{d}{dt} [\text{COOH}] = -k[\text{COOH}][\text{GM}]$$

Above, $[\text{GM}]$ refers to the concentration of glycidyl methacrylate. The equation can be integrated by assuming the stoichiometric relation between $[\text{GM}]$ and $[\text{COOH}]$, and the plot in Figure 6 shows a considerable deviation from the experimental result. This suggests that the first-order plot is a better representation of the experimental data.

Step 3: Preparation of "COMB" graft copolymer disperant

A feed mixture of MMA (24.02 g), methacrylic acid (0.49 g), poly(12-hydroxystearic acid), and the adduct

**Figure A.4** The boiling characteristics of the petrol used in our studies.

solution prepared in step 2 (48.03 g) was prepared. In one shot, the ethyl acetate and butylacetate mixture (in a 2 : 1 ratio) were charged to a reactor at 80°C. After 5–10 min of the initial charge, the feed mixture was introduced at a constant rate over a period of 3 h. After the addition was complete, the total charge was maintained at 80°C for a further 2 h.

If at any stage the copolymer precipitates from the solvent, it was found that it could never be dissolved again. Through experimentation we found that a 2 : 1 mixture of ethyl acetate and butyl acetate gives the correct medium for the copolymer formation. If we added the monomer mixture simultaneously at the starting time, the copolymer had the tendency to precipitate. As a result, we added the mixture of monomers slowly over a period of 3 h. The inability of the grafted copolymer to return back to solution after precipitation can be explained by the fact that branched pendant chains of poly(hydroxystearic acid) become entangled on precipitation. These now do not open up even when the correct solvancy is restored.

APPENDIX II

Characterization of Petrol Used for Dispersion Polymerization

Petrol is a mixture of several hydrocarbons and it can be characterized by its boiling and flash-point characteristics as follows:

Boiling characteristics of petrol were determined by distilling it. One hundred milliliters of it was placed in a round-bottom flask and heated slowly. The vapors were condensed and collected in a measuring cylinder. The temperature of the flask was noted against the volume collected in the intervals of 5 mL. The temperature of the flask when the first drop of the vapor condenses is known as the initial boiling point. The temperature vs. volume data is plotted in Figure A.4.

Flash Point

The flash point of petrol was found using a Pensky Martens apparatus. The required amount of it was taken in the apparatus and heated slowly using a burner with continual stirring. A small test flame was directed into the end at regular intervals with a simultaneous interruption of stirring. The flash point is taken as the lowest temperature at which the applications of the test flame causes the vapor above the sample to ignite momentarily. The flash point of the petrol used was 47°C.

REFERENCES

1. D. K. Walbridge, *Polymerization in Nonaqueous Dispersions in Comprehensive Polymer Science*, G. Allen and J. C. Bevington, Eds., Pergamon, 1989, Vol. 4, p. 243.
2. K. E. J. Barrett, *Dispersion Polymerization in Organic Media*, Wiley, London, 1975.
3. D. C. Blackley, *Emulsion Polymerization, Theory and Practice*, Applied Science, London, 1975.
4. W. Hubinger and K. H. Reichert, in *Modelling of Inverse Polymerization of Acrylamide in Polymer Reaction Engineering*, K. H. Edicher and W. Geiseler, Eds., V. C. H., 1989.
5. A. J. Paine, *J. Polym. Sci. Polym. Chem.*, **28**, 2485 (1990).
6. M. H. Litt, C. S. Lin, and I. M. Krieger, *J. Polym. Sci. Polym. Chem.*, **28**, 2777 (1990).
7. S. K. Saha and A. K. Chaudhury, *J. Polym. Sci. Polym. Chem.*, **25**, 519–532 (1987).
8. V. Glukhikh, C. Graikat, and C. Pichot, *J. Polym. Sci. Polym. Chem.*, **25**, 1127–1162 (1987).
9. C. K. Ober and M. L. Hair, *J. Polym. Sci. Polym. Chem.*, **25**, 1895–1908 (1987).
10. C. Gaikat, C. Pichot, A. Guyot, and M. S. El Aasser, *J. Polym. Sci. Polym. Chem.*, **24**, 427–450 (1986).
11. A. Bukowski and B. Liszynska, *J. Appl. Polym. Sci.*, **31**(1), 283–290 (1986).
12. Y. Y. Lu, M. S. El Asser, and J. W. Vanderhoft, *J. Polym. Sci. Polym. Phys.*, **26**, 1187–1204 (1988).
13. E. B. Nauman, S.-T. Wang, and N. P. Balsara, *Polymer*, **27**, 1637–1640 (1986).
14. F. A. Bovey, I. M. Kolthoff, A. I. Medalia, and E. J. Meehan, *Emulsion Polymerization*, 1st ed., Wiley-Interscience, New York, 1955.
15. G. S. Hartley, *Aqueous Solutions of Paraffin-Chain Salts*, 1st ed., Hermann, Paris, 1936.
16. K. W. Min and W. H. Ray, *J. Macromol. Sci. Rev. Macromol. Chem.*, **C11**, 177 (1974).
17. T. Mastsumoto, in *Emulsion and Emulsion Technology*, 1st ed., K. J. Lissant, Ed., Marcel Dekker, New York, 1974, Part II.
18. W. Cooper, in *Reactivity, Mechanism and Structure in Polymer Chemistry*, 1st ed., A. D. Jenkins and A. Ledwith, Eds., Wiley, New York, 1974.
19. D. R. Bassett and A. E. Hamielec, Eds., 1st ed., *Emulsion Polymers and Emulsion Polymerization*, ACS Symp. Ser. 165, American Chemistry Society, Washington, DC, 1982.
20. I. Piirma, *Emulsion Polymerization*, 1st ed., Academic Press, New York, 1982.
21. R. B. Bird, W. E. Stewart, and E. N. Lightfoot, *Transport Phenomena*, Wiley, New York, 1960.
22. J. Ugelstad, P. C. Mork, P. Dahl, and P. Rangnes, *J. Polym. Sci. Part C*, **27**, 49 (1969).
23. G. Lichti, R. G. Gilbert, and D. H. Napper, *J. Polym. Sci. Polym. Chem.*, **15**, 1957 (1977).
24. K. H. Reichert and H. U. Moritz, *Makromol. Chem. Macromol. Symp.*, **10/11**, 571 (1987).
25. C. K. Uranek, *Rubber Chem. Tech.*, **49**, 610 (1976).
26. J. Ugelstad and F. K. Hansen, *Rubber Chem. Tech.*, **49**, 536 (1976).
27. P. Bataille, B. T. Van, and Q. B. Pham, *J. Polym. Sci. Polym. Chem.*, **20**, 795 (1982).
28. Z. Song and G. W. Pohlein, *J. Macromol. Sci.-Chem*, **A25**, 403 (1988).

Received June 24, 1992

Accepted October 30, 1992